Acta Crystallographica Section D
Biological Crystallography
ISSN 0907-4449

Effects of microgravity on the crystal quality of a collagen-like polypeptide

R. Berisio,[a] L. Vitagliano,[a] G. Sorrentino,[a] L. Carotenuto,[b] C. Piccolo,[b] L. Mazzarella[a] and A. Zagari[a]*

[a]Centro di Studio di Biocristallografia, CNR and Dipartimento di Chimica, Università di Napoli 'Federico II', Via Mezzocannone 4, 80134 Napoli, Italy, and [b]Microgravity Advanced Research and Support Center (MARS), Via Comunale Tavernola, 80144 Napoli, Italy

Correspondence e-mail: zagari@chemna.dichi.unina.it

Received 14 August 1999
Accepted 2 November 1999

(Pro-Pro-Gly)$_{10}$ is one of the most widely studied collagen polypeptide models. Microgravity crystal growth of (Pro-Pro-Gly)$_{10}$ was carried out in the Advanced Protein Crystallization Facility aboard the Space Shuttle Discovery during the STS-95 mission. Crystals were successfully grown in all experiments, using both dialysis and free-interface diffusion methods. The quality of the microgravity-grown crystals and of ground-grown counterparts was assessed by X-ray synchrotron diffraction. Microgravity-grown crystals exhibited a significant improvement in terms of dimensions and resolution limit. As previously reported, crystals were orthorhombic, space group $P2_12_12_1$. However, the diffraction pattern showed weak reflections, never previously measured, that were consistent with new unit-cell parameters a = 26.9, b = 26.4, c = 182.5 Å. This allowed the derivation of a new model for the arrangement of the triple-helical molecules in the crystals.

1. Introduction

Collagen is the most abundant protein in vertebrates and is a fundamental component of several connective tissues (Nimni, 1988). Its peculiar structural motif, known as the triple helix, is a common feature among the most abundant types of collagen. Owing to its fibrous nature, detailed structural information on native collagen is rather limited. Indeed, only low-resolution models have been derived from X-ray fibre diffraction (Fraser *et al.*, 1979). The commonly accepted collagen model consists of three super-coiled polyproline II-like chains, requiring Gly at every third residue (*X*-*Y*-Gly), with the *X* and *Y* positions frequently occupied by imino acids. Important information about the structure stability and functionality of the collagen triple helix has been obtained in studies on polypeptide models (Bella *et al.*, 1994; Yang *et al.*, 1997; Holmgren *et al.*, 1998; Kramer *et al.*, 1998 and references therein), (Pro-Pro-Gly)$_{10}$ (PPG$_{10}$) being one of the most widely studied synthetic collagen models. The first structural investigation of this polypeptide dates back to the early 1970s (Sakakibara *et al.*, 1972), when the peculiar diffraction pattern of (PPG)$_{10}$, with its occurrence of very strong and very weak reflections, was identified. Reflections were indexed according to an orthorhombic system, with unit-cell parameters a = 26.9, b = 26.4, c = 101.4 Å; the strong reflections indicated the existence of a sub-cell with c' = 20.2 Å. Using only the strong reflections, a low-resolution model was then obtained assuming an infinite peptide molecule (Okuyama *et al.*, 1981). Recently, together with H. M. Berman's group, we derived a detailed description of the infinite model and its interactions with solvent molecules (Kramer *et al.*, 1998), using two independent sets of high-resolution data. Some of our findings, mainly regarding the polypeptide hydration, have been

Table 1
Final crystallization conditions in APCF reactors.

Reactor type	No.	Final composition				
		$(PPG)_{10}$ (mg ml^{-1})	Sodium acetate (*M*)	Acetic acid (*M*)	PEG 400 [%(*v*/*v*)]	ΔPEG† [%(*v*/*v*)]
DIA	5	5.0	0.19–0.22	0.04	10.0–10.5	0–2
FID	2	4.5	0.22	0.04	8.9–9.5	2–5

† ΔPEG stands for the difference in PEG 400 concentration between the protein and the precipitant chambers.

questioned by an independent structure determination (Nagarajan *et al.*, 1998); an indication that, after almost three decades of structural investigation, some aspects still deserve further analysis.

Very accurate X-ray data are necessary to obtain a thorough description of the structure and hydration pattern of $(PPG)_{10}$. In order to obtain well diffracting crystals which would allow also the measurement of the weak extra reflections, we grew the crystals in microgravity.

Microgravity has improved crystal quality in several cases by reducing convection effects and sedimentation. Indeed, by reducing buoyancy forces, microgravity is thought to lead to a more stable depletion layer around the crystal, thus favouring more regular growth (McPherson, 1993; Rosenberger *et al.*, 1996; Chayen *et al.*, 1997; Lorber *et al.*, 1999). Comparative studies of space- and ground-grown crystals have shown that in many cases microgravity-grown crystals exhibit a significant quality improvement, namely in size, resolution limits and mosaicity (Esposito *et al.*, 1998; McPherson *et al.*, 1999).

In other cases, however, no improvements were observed, thus leading to arguments questioning the benefits of microgravity on protein crystal growth (Couzin, 1998; Chayen & Helliwell, 1999). It is difficult to draw conclusions in this debate. Indeed, a great number of factors need to be considered, such as the jitters of the mission, the crystallization method and facility as well as the specific protein and its physicochemical properties. For example, the molecular shape and volume of the protein and the diffusibility of the components in the crystallizing mixture may affect the crystal growth significantly. As a result, microgravity as a method of improving crystal growth has not yet been fully exploited.

So far, only globular proteins have been studied and, in this framework, we recently investigated the effect of microgravity on the growth of alcohol dehydrogenase crystals (Esposito *et al.*, 1998). $(PPG)_{10}$ is a new case study, since it is the first fibre-like system to be crystallized under microgravity conditions and therefore provides new clues about the feasibility of crystallization in microgravity for non-globular proteins. The results of this investigation are described in this paper. Using microgravity-grown crystals, we were able to collect data to 1.3 Å resolution, which represents the highest resolution limits thus far attained. A large fraction of the extra reflections were measured and these data allowed us to derive new unit-cell parameters and propose a new model for the packing of $(PPG)_{10}$ molecules, which involves a head-to-tail interaction of the triple helices.

2. Materials and methods

2.1. Pre-flight experiments

The conditions reported by Kramer *et al.* (1998) were adapted to other crystallization techniques, such as dialysis and free-interface diffusion. Preliminary crystallization trials, using free-interface diffusion (FID) and dialysis (DIA), produced only needles and very small plates (with a maximum dimension of 0.02 mm), respectively. The addition of PEG 400 improved the results significantly. Indeed, crystals with maximum dimensions of 0.2–0.3 mm were obtained using dialysis with a final $(PPG)_{10}$ concentration of 5.0 mg ml^{-1} in 0.04 *M* acetic acid, 0.22 *M* sodium acetate, 10%(*v*/*v*) PEG 400. FID produced small crystals, with a maximum dimension of 0.05 mm, using a final $(PPG)_{10}$ concentration of 4.5 mg ml^{-1} in 0.05 *M* acetic acid, 0.22 *M* sodium acetate, 10%(*v*/*v*) PEG 400. The crystallization conditions found were then optimized in the Advance Protein Crystallization Facility (APCF) FID reactors which were used in both the FID and the DIA configurations. Since the duration of the flight was 8 d, particular attention was given to the time period needed to grow sufficiently large crystals. During these preparatory trials, crystals appeared within 24 h and reached dimensions of 0.2–0.3 mm in about one week.

2.2. Microgravity experiments

Microgravity experiments were carried out in seven reactors (five DIA and two FID) under the conditions listed in Table 1. Ground controls were carried out simultaneously, with identical materials in identical apparatus and under identical temperature conditions. The volume of the protein chamber was 55 and 67 µl for the DIA and FID reactors, respectively. All of the reactors were filled in the laboratory of Dr C. Betzel in Hamburg, Germany. The space reactors were integrated in the APCF and transported to the launch site at the Kennedy Space Center (KSC), USA. An APCF unit provides a total of 48 individual crystallization cells maintained at a constant temperature (in this case, 291 ± 1 K). The APCF was flown aboard the Space Shuttle Discovery during the STS-95 mission (October 1998) and all the reactors were activated after a microgravity environment was achieved and were deactivated before re-entry. Both the DIA and the FID reactors were activated by a 90° rotation of a stopcock valve that establishes continuity between the protein and precipitant chambers. In four reactors, crystal growth was monitored using a CCD video at time intervals throughout the flight.

2.3. Data collection and processing

Microgravity and ground-control crystals were analysed using synchrotron radiation at Elettra, Trieste, Italy and at the DORIS storage ring, DESY, Hamburg, Germany. Data were recorded on a MAR Research image-plate detector at room temperature, since all attempts to find a cryo-protectant were unsuccessful. Because crystals decayed in the X-ray beam, a total of ten crystals (five microgravity- and five ground-grown ones) were used for data collection. Two data collections, for

low (15.0–1.9 Å resolution) and high (15.0 Å to highest resolution) resolution, were carried out for both microgravity- and ground-grown crystals. In order to compare crystal quality, the same exposure, crystal-to-detector distance and oscillation angle were used for both microgravity- and ground-grown crystals. All data were processed using the *HKL* package (Otwinowski & Minor, 1997).

3. Results and discussion

3.1. Pre-flight results

Crystals diffracting to 1.7 and 2.0 Å were obtained under two different conditions using the hanging-drop vapour-diffusion method (Kramer *et al.*, 1998). In both cases, the slow pH increase arising from the vapour diffusion of acetic acid from the drop to the reservoir seemed to be the main driving force for crystallization.

To prepare the flight experiment, ground experiments were carried out in the Advanced Protein Crystallization Facility (APCF; Bosch *et al.*, 1992; Snell *et al.*, 1996). Although its original configuration included the vapour-diffusion hanging-drop and sitting-drop techniques, since they are the most widely used on Earth, the APCF presently allows only FID and DIA. These last two methods have produced the best results in the various space-shuttle missions (Boggon *et al.*, 1998; Esposito *et al.*, 1998; Chayen & Helliwell, 1999). Under these circumstances, we adapted vapour-diffusion crystallization conditions previously used for $(PPG)_{10}$ (Kramer *et al.*, 1998) to DIA and FID.

The use of the same crystallizing solutions as in vapour diffusion led only to needles and small plates, most likely because of the rapid pH increase which occurs when using dialysis and free-interface diffusion compared with vapour diffusion. The addition of PEG 400 improved the results significantly. Crystallization trials were carried out both in laboratory devices and in the APCF and comparable results were obtained. In all trials, dialysis led to better results (crystals of maximum dimension 0.2 mm) compared with free-interface diffusion, where only microcrystals were obtained.

3.2. Post-flight results: crystal features

We carried out crystallization experiments on $(PPG)_{10}$ during the STS-95 Spacelab mission of the Space Shuttle Discovery, which was launched on 29 October and returned on 7 November, 1998. The compositions of the crystallizing solutions used are listed in Table 1.

The reactors were inspected immediately after the flight's return and crystals were found in all the reactors. Microgravity produced better results in terms of crystal size in nearly all cases. Furthermore, as already observed during the pre-flight experiments, DIA gave a smaller number of crystals with larger dimensions than FID. This was observed both in microgravity and on the ground.

Using dialysis, we obtained five microgravity-grown crystals with a maximum dimension in the range 0.35–0.55 mm and a few smaller crystals (0.05–0.20 mm). By contrast, only one terrestrial crystal had a maximum dimension larger than 0.3 mm (0.35 mm), while many smaller crystals (0.05–0.15 mm) were obtained. As a typical example, Fig. 1 shows a comparison between microgravity- and ground-grown crystals obtained in the same crystallization medium using dialysis. A close-up of a single microgravity-grown crystal is also shown (Fig. 1*c*). Similarly, crystals grown using FID reached a maximum dimension of 0.05 mm in microgravity, whereas only a microcrystalline precipitate was obtained on the ground.

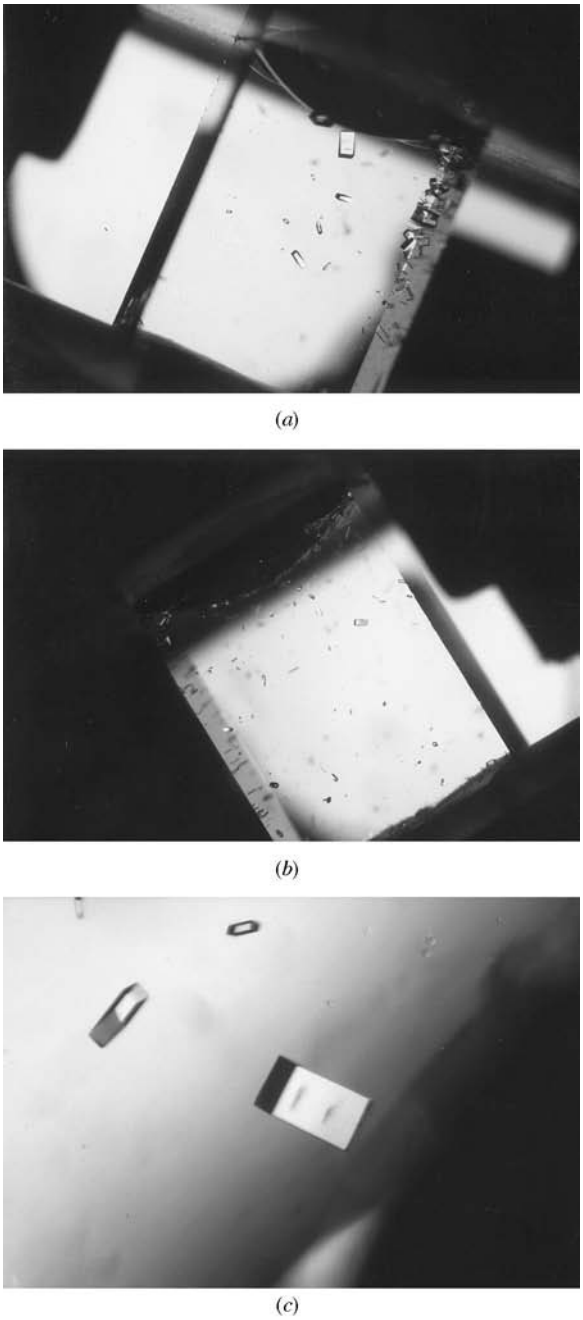

Figure 1
A comparison of crystals grown in DIA reactors in (*a*) microgravity conditions and (*b*) on Earth; (*c*) a close-up view of a crystal grown in microgravity.

3.3. Checking the highest resolution limits

Several microgravity- and ground-grown crystals were tested in order to assess the quality of the diffraction pattern. We found that numerous microgravity-grown crystals obtained using dialysis showed diffraction to 1.2 Å, while only the largest ground-control crystal reached this resolution. The remaining ground-grown crystals were, in fact, significantly smaller (<0.2 mm) and diffracted to a maximum resolution of 1.7 Å. When crystals of similar size were analysed, microgravity-grown crystals showed higher resolution limits in most cases. Finally, microgravity-grown crystals obtained using FID showed diffraction to 1.7 Å, while no crystals suitable for data collection were grown on the ground.

3.4. Statistics and comparisons

Using the same data-collection experimental setup and the same number of crystals, we collected data which extended to 1.3 Å for the microgravity-grown crystals and to 1.6 Å for the ground-grown crystals. The resolution limit gained for the microgravity-grown crystals is the highest thus far obtained for a collagen-like polypeptide (Bella *et al.*, 1994; Kramer *et al.*, 1998, Nagarajan *et al.*, 1998).

3.4.1. The sub-cell. $(PPG)_{10}$ is characterized by a peculiar diffraction pattern with an uneven distribution of the reflection intensities; most of the strongest reflections correspond to a sub-cell with a *c* axis of about 20 Å. Previously, since it was not possible to obtain an accurate measurement of the weak extra reflections, only the reflections characterizing the sub-cell were considered for $(PPG)_{10}$ structure determination. This led to a model that behaved as an infinite chain (Kramer *et al.*, 1998; Nagarajan *et al.*, 1998).

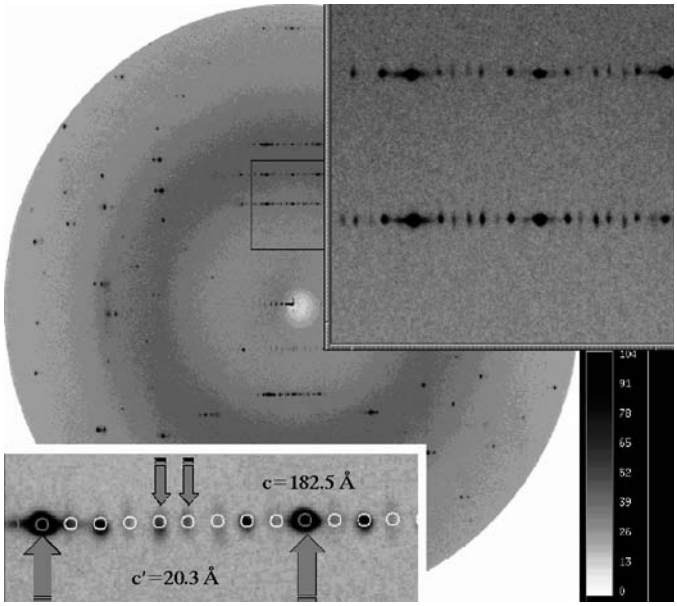

Figure 2
Diffraction image from a microgravity-grown crystal. The bottom-left icon shows the predicted reflections: reflections characterizing the sub-cell and the newly found unit cell are indicated by large and small arrows, respectively.

Table 2
Data-processing statistics.

	Microgravity	Ground
Space group	$P2_12_12_1$	$P2_12_12_1$
Sub-cell		
Unit-cell parameters (Å)		
a'	26.9	26.9
b'	26.3	26.4
c'	20.3	20.3
Resolution range (Å)	15.0–1.3	15.0–1.6
Multiplicity	4.8	3.3
Completeness (%)	90.9† (91.6‡)	85.4‡
Last shell	66.4§	77.2¶
R_{merge} (%)	4.2† (4.0‡)	4.5‡
Last shell	9.3§	12.0¶
Large cell		
Unit-cell parameters (Å)		
a	26.9	26.9
b	26.4	26.4
c	182.5	182.6
Resolution range (Å)	15.0-1.3	15.0-1.6
Multiplicity	4.7	2.8
Mosaicity	0.65–0.85	0.65–0.88
Completeness (%)	89.8† (90.0‡)	82.3‡
Last shell	66.8§	60.2¶
R_{merge} (%)	9.9† (9.0‡)	5.1‡
Last shell	19.5§	33.6¶

† Resolution range: 15.0–1.33 Å. ‡ Resolution range: 15.0–1.75 Å. § Resolution range: 1.33–1.30 Å. ¶ Resolution range: 1.75–1.60 Å.

First, we processed the data from both microgravity- and ground-grown crystals, taking into account only the reflections characterizing the sub-cell; statistics are reported in Table 2 and R_{merge} was comparable in spite of the different resolution limit. This processing was aimed at comparing the quality of the strongest reflections diffracted by the microgravity and ground-grown crystals, as well as obtaining an improved quality data set which can provide a more detailed description of the infinite model.

Data quality for the ground-grown crystals was similar to that obtained previously (Kramer *et al.*, 1998), in terms of R_{merge} and completeness. In fact, 1781 reflections, with 86.5% having $\langle I/\sigma(I)\rangle > 3$, were measured for the ground-grown crystals to 1.6 Å resolution. In contrast, space-grown crystals yielded as many as 93.6% more intensities [3448 reflections up to 1.3 Å, with 95.0% having $\langle I/\sigma(I)\rangle > 3$] than the control crystals grown on Earth. The markedly higher number of observations obtained for the microgravity data will provide significantly more accurate structural information about $(PPG)_{10}$. Hopefully, a deeper insight will be gained into the interactions of $(PPG)_{10}$ with water molecules in relation to collagen stability and the puckering of the proline rings, two topics which have been debated recently (Holmgren *et al.*, 1998; Nagarajan *et al.*, 1998).

3.4.2. Interpreting the whole diffraction pattern. Analyses of the diffraction images revealed a surprising feature. The indexing of many extra reflections consistently revealed a *c* axis (c = 182.5 Å; Table 2) much larger than previously believed (Okuyama *et al.*, 1981; Kramer *et al.*, 1998; Nagarajan *et al.*, 1998). Indeed, in all the previous studies conducted on crystals obtained under similar conditions, only a small frac-

Table 3
Resolution limits of the classes of reflection.

l index	$9n$	$9n+1$	$9n+2$	$9n+3$	$9n+4$	$9n+5$	$9n+6$	$9n+7$	$9n+8$
Microgravity d (Å)	1.3	1.7	1.3	4.0	1.7	2.8	3.0	1.7	3.2
Ground d (Å)	1.6	2.4	1.6	3.7	2.0	2.8	3.0	2.4	3.2

tion of extra reflections were measured and these very weak reflections were tentatively indexed with c = 101.4 Å.

Fig. 2 shows an example of a diffraction image recorded on a microgravity-grown crystal and the corresponding indexing. Reflections can be classified into nine classes, depending on the l index; the reflections defining the sub-cell correspond to the class with $l = 9n$. The presence of the sharp satellite reflections (with $l = 9n + 2$ and $l = 9n - 2$) made the indexing unambiguous for both microgravity (Fig. 2) and ground-grown crystals.

Data-processing statistics show that a higher resolution, completeness and multiplicity were obtained for crystals grown in microgravity (Table 2). Compared with the sub-cell statistics, where only $l = 9n$ reflections were used, the microgravity data set shows a higher $R_{\rm merge}$. This is ascribed to the higher incidence of the weak reflections with $l \neq 9n$, which are more intense in the microgravity set. The higher value of $R_{\rm merge}$ for the data set from microgravity-grown crystals is a consequence of a higher frequency of the measured reflections with $l \neq 9n$.

The same number of crystals (five microgravity- and five ground-grown crystals) was used for data collection. All the microgravity-grown crystals, however, diffracted to 1.3 Å, while only the largest ground-grown crystal showed this resolution limit. The other four crystals only diffracted to 1.7 Å. As both microgravity and ground-grown crystals showed some decay, data are only complete to 1.33 and 1.75 Å for microgravity- and ground-grown crystals, respectively (Table 2).

An estimate of the crystal mosaicity, derived from *SCALEPACK* (Otwinowski & Minor, 1997), does not show significant differences between the crystals. However, a better comparison of mosaicities would have required a more accurate analysis of the reflection profile.

A comparative analysis of data from microgravity-grown crystals and ground-control crystals was carried out for each of the nine reflection classes which characterize the diffraction pattern of $(PPG)_{10}$.

As shown in Fig. 3, reflections belonging to the nine reflection classes have markedly different intensities: those with $l = 9n$ and $l = 9n + 2$ are the strongest, followed by those with $l = 9n + 4$ and $l = 9n + 7$. The reflections belonging to the other five reflection classes are extremely weak, less than 30.8% having $\langle I/\sigma(I)\rangle > 3$. Moreover, microgravity crystals have comparable $\langle I/\sigma(I)\rangle$ values at low resolution, while a strong decrease of $\langle I/\sigma(I)\rangle$ is observed for the ground-grown crystals at a resolution higher than 1.8 Å.

Reflections belonging to different classes diffracted to different resolution levels and a resolution limit was associated with each class. The highest resolution shell was taken as the last shell with at least 50% of the reflections having $\langle I/\sigma(I)\rangle > 3$. Resolution limits for the nine classes, for both microgravity- and ground-grown crystals, are reported in Table 3.

The table shows, for both microgravity- and ground-grown crystals, that reflections with $l = 9n$ and $l = 9n + 2$ show the crystal's highest resolution limits. Moreover, together with these two classes, reflections with $l = 9n + 1$, $9n + 4$ and $9n + 7$ show lower resolution limits in the set from ground-grown crystals. This is in accordance with the slightly higher $\langle I/\sigma(I)\rangle$ ratio measured for the microgravity-grown crystals.

3.5. A new model for crystal packing of $(PPG)_{10}$

The increased diffraction power of microgravity crystals and the better definition of the extra reflections have permitted an improved determination of the unit-cell parameters. The results clearly indicate that the crystal repetition along the c axis has a value of 182.5 Å, not 101.3 Å as originally suggested by Okuyama *et al.* (1981) and confirmed by other authors (Kramer *et al.*, 1998; Nagarajan *et al.*, 1998). This modified value of the c axis, which is parallel to the molecular helical axis, suggests a new model for the packing of the discrete polypeptide molecules in the crystal. On the basis of the previously refined model (Kramer *et al.*, 1998), the unit height for each of the three single 7_1 helices which are wrapped around a common axis to form the triple helix is 8.7 Å. Considering that the three helices are staggered within the triple-helical structure, this aggregate is expected to be about 90 Å long, a value which closely corresponds to half the c axis. We propose that in the crystal these triple-helical molecules are packed on top of each other in a head-to-tail fashion. According to this model, within one repeat unit along the c axis the crystal contains a series of blocks, 20.3 Å long, having a potentially perfect triple-helical arrangement, interrupted by blocks where the charged C- and N-terminal residues of two adjacent molecules interact.

The solvent content of $(PPG)_{10}$ crystals was previously calculated by Sakakibara *et al.* (1972). On the basis of the observed density of the crystals (1.31 g cm^{-3}), these authors found a water content of 46%. Using the new value of the unit-cell parameters and assuming two molecules in the asymmetric unit, we calculated V_m = 2.13 Å^3 Da^{-1}, compared with the V_m = 2.40 Å^3 Da^{-1} previously obtained. A significantly lower solvent content (40%) was found, which is in accordance with the head-to-tail model in the crystal, in which only the lateral assembly of the triple-helical moieties is mediated by solvent molecules.

The proposed model is characterized by a direct interaction between the charged C-terminal and N-terminal residues of adjacent molecules across the helical axis. This feature accounts well for the pH-dependence of the solubility of $(PPG)_{10}$, which markedly decreases on moving from acidic to neutral pH. The head-to-tail model, in fact, suggests that

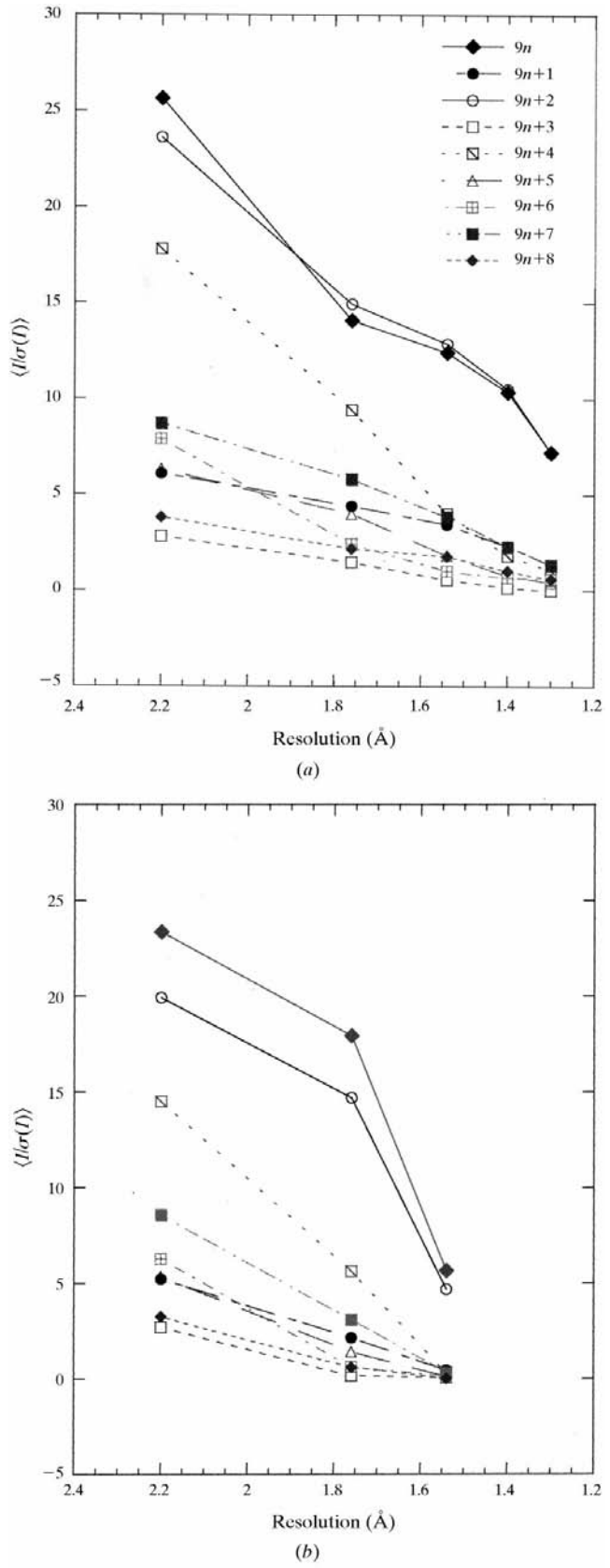

Figure 3
$\langle I/\sigma(I)\rangle$ *versus* resolution for each of the nine reflection classes, calculated for the data set from (*a*) microgravity-grown and (*b*) ground-grown crystals.

aggregation of the molecules is favoured when both N- and C-termini are charged.

4. Conclusions

All the microgravity experiments produced a smaller number of crystals compared with the ground-control experiments. This finding presumably originated from a smaller number of nuclei in the bulk solution, thus indicating that the kinetics of the super-saturation were different.

In microgravity, nuclei grew to a larger size. This may result from either a larger number of nutrient molecules (when a smaller number of nuclei is formed) or a minor accumulation of impurities, which often stifles growth. These favourable conditions may be generated by the depletion zone established around growing crystals (McPherson *et al.*, 1999).

Microgravity-grown crystals diffracted X-rays to a higher resolution. Only the largest ground-grown crystal diffracted to 1.3 Å, while improvements in resolution (from 1.7 to 1.3 Å) were consistently measured from a dozen crystals grown in microgravity in the DIA reactors. This effect has been observed to some degree in many space-shuttle missions (McPherson *et al.*, 1999 and references therein; Boggon *et al.*, 1998 and references therein). The increase of the resolution limits is likely to be partly a consequence of the larger size of the microgravity-grown crystals. However, improvements of the resolution limits were also frequently observed for crystals of similar size, thus indicating a minor overall statistical disorder for the microgravity-grown crystals.

Up to now, microgravity studies have been carried out on globular proteins. Our results provide evidence that the benefits of microgravity can be extended to non-globular proteins.

In addition, the increased diffracting power of the microgravity crystals was very helpful for the correct determination of the $(PPG)_{10}$ unit-cell parameters, which were incorrectly determined in all previous analyses since only a small fraction of the weak extra reflections could be registered (Okuyama *et al.*, 1981; Kramer *et al.*, 1998; Nagarajan *et al.*, 1998). Based on the new unit-cell parameters, we derived a model for the packing of $(PPG)_{10}$ molecules which involves a direct head-to-tail interaction of the charged N- and C-termini of the triple helices. A similar organization of the molecules is also likely to occur for other synthetic polypeptides with free charged extremities. For example, $(Pro\text{-}Hyp\text{-}Gly)_{10}$ shows a similar diffraction pattern as $(PPG)_{10}$ and so far no model for the arrangement of the molecules in the crystals has been proposed (Nagarajan *et al.*, 1999). Moreover, microgravity has provided a set of high-resolution data which could resolve some questions (Bella *et al.*, 1995; Kramer *et al.*, 1998; Nagarajan *et al.*, 1998; Holmgren *et al.*, 1998) regarding collagen structure and stability.

We acknowledge the European Space Agency (Dr H. U. Walter, Dr O. Minster and P. Di Palermo) for providing the flight opportunity, Dr R. Bosch and Dr P. Lautenschlager

(Dornier, GmbH, Friedrichshafen, Germany) for assistance with the APCF reactors, Dr C. Betzel (DESY, Hamburg, Germany) for excellent hospitality in his laboratory, Dr R. Z. Kramer for helpful discussions and M. Amendola for technical assistance. We acknowledge EMBL/DESY for beam time and support, and the Sincrotrone Trieste and CNR Staff at Elettra, Trieste (Italy) for their help in the use of the Facility supported by Elettra Experimental Division and by CNR and Elettra Scientific Division. This work was financially supported by the Agenzia Spaziale Italiana.

References

Bella, J., Brodsky, B. & Berman, H. M. (1995). *Structure*, **3**, 893–906.
Bella, J., Eaton, M., Brodsky, B. & Berman, H. M. (1994). *Science*, **266**, 75–81.
Boggon, T. J., Chayen, N. E., Snell, E. H., Dong, J., Lautenschlager, P., Potthast, L., Siddons, D. P., Stojanoff, V., Gordon, E., Thompson, A. W., Zagalsky, P. F., Bi, R.-C. & Helliwell, J. R. (1998). *Philos. Trans. R. Soc. London Ser. A*, **356**, 1045–1061.
Bosch, R., Lautenschlager, P., Potthast, L. & Stapelmann, J. (1992). *J. Cryst. Growth*, **122**, 310–316.
Chayen, N. E., Boggon, T. J., Cassetta, A., Deacon, A., Gleichmann, T., Habash, J., Harrop, S. J., Helliwell, J. R., Nieh, Y. P., Peterson, M. R., Raftery, J., Snell, E. H., Hädener, A., Niemann, A. C., Siddons, D. P., Stojanoff, V., Thompson, A. W., Ursby, T. & Wulff, M. (1996). *Quart. Rev. Biophys.* **29**, 227–278.
Chayen, N. E. & Helliwell, J. R. (1999). *Nature (London)*, **398**, 20.
Chayen, N. E., Snell, E. H., Helliwell, J. R. & Zagalsky, P. F. (1997). *J. Cryst. Growth*, **171**, 219–225.
Couzin, J. (1998). *Science*, **281**, 497–498.
Esposito, L., Sica, F., Sorrentino, G., Berisio, R., Carotenuto, L., Giordano, A., Raia, C., Rossi, M., Lamzin, V. S., Wilson, K. S. & Zagari, A. (1998). *Acta Cryst.* D**54**, 386–390.
Fraser, R. D. B., MacRae, T. P. & Suzuki, E. (1979). *J. Mol. Biol.* **129**, 463–481.
Holmgren, S. K., Taylor, K. M., Bretscher, L. E. & Raines, R. T. (1998). *Nature (London)*, **392**, 666–667.
Kramer, R. Z., Vitagliano, L., Bella, J., Berisio, R., Mazzarella, L., Brodsky, B., Zagari, A. & Berman, H. M. (1998). *J. Mol. Biol.* **280**, 623–638.
Lorber, B., Sauter, C., Robert, M. C., Capelle, B. & Geigé, R. (1999). *Acta Cryst.* D**55**, 1491–1494.
McPherson, A. (1993). *J. Phys. D*, **26**, B104–B112.
McPherson, A., Malkin, A. J., Kutznetsov, Y. J., Koszelak, S., Wells, M., Jenkins, G., Howard, J. & Lawson, G. (1999). *J. Crystal Growth*, **196**, 572–586.
Nagarajan, V., Kamitori, S. & Okuyama, K. (1998). *J. Biochem.* **124**, 1117–1123.
Nagarajan, V., Kamitori, S. & Okuyama, K. (1999). *J. Biochem.* **125**, 310–318.
Nimni, M. E. (1988). Editor. *Collagen*, pp. 1–4. Boca Raton, Florida: CRC.
Okuyama, K., Okuyama, K., Arnott, S., Takayanagi, M. & Kakudo, M. (1981). *J. Mol. Biol.* **152**, 427–443.
Otwinowski, Z. & Minor, W. (1997). *Methods Enzymol.* **276**, 307–326.
Rosenberger, F., Vekilov, P. G., Muschol, M. & Thomas, B. R. (1996). *J. Cryst. Growth*, **168**, 1–27.
Sakakibara, S., Kishida, Y., Okuyama, K., Tanaka, N., Ashida, T. & Kakudo, M. (1972). *J. Mol. Biol.* **65**, 371–373.
Snell, E. H., Helliwell, J. R., Boggon, T. J., Lautenschlager, P. & Potthast, L. (1996). *Acta Cryst.* D**52**, 529–533.
Yang, W., Chan, V. C., Kirkpatrick A., Ramshaw, J. A. M. & Brodsky, B. (1997) *J. Biol. Chem.* **272**, 28837–28840.